

## Improved hygrothermal performance of rigid foams using natural fibers and 2,5-dihydroxymethyl furan bonded to carbohydrate chains

Lionel Tapsia Karga<sup>a\*</sup>, Noel Konai<sup>b</sup>, Maxime Dawoua Kaoutoing<sup>a</sup>, Benoit Ndiwe<sup>c</sup>, Tawe Lynde<sup>d</sup>, Monabeng Claire<sup>g</sup>, Achille Gnassiri Wedaina<sup>d,f</sup>, Nzogning Fotio Arnaud<sup>c</sup>, and Raidandi Danwe<sup>g</sup>.

<sup>a</sup>National Advanced School of Mines and Petroleum Industries, University of Maroua, Kaélé, P.O. Box 08 Kaélé, Cameroon.

<sup>b</sup>Laboratory of Civil Engineering and Mechanical, National Advanced School of Engineering, University of Yaounde 1, BP 8390, Yaoundé, Cameroon.

<sup>c</sup>Higher Technical Teacher Training College Douala, University of Douala, P.O. Box 2701, Douala, Littoral Region, Cameroon.

<sup>d</sup>Department of Wood Construction, University Institute for Wood Technology, University of Yaounde 1, Yaounde, Cameroon.

<sup>e</sup>Laboratory of Mechanics, Materials, and Modelization (PAI), University of Ngaoundéré, P.O. Box, 454 Ngaoundéré, Cameroon.

<sup>f</sup>CFPE-Professional Training Center of Douala, Cameroon.

<sup>g</sup>Laboratory of Materials, Architecture and Civil Engineering, National Advanced School of Engineering, University of Maroua, BP 46, Maroua, Cameroon.

### ABSTRACT

This work aimed to evaluate the particle content of fibers in rigid foams made from *Monopetalantus* tannin. *Monopetalantus* tannin, sugarcane bagasse fibers, raffia bamboo cork fibers and bio-hardener were extracted and used to formulate foams with different proportions of reinforcement (by mixing the different reagents). The foams produced were characterized. The apparent densities of the foams produced varied between 0.08 g/cm<sup>3</sup> and 0.47 g/cm<sup>3</sup> and it was noted that the density increased with the proportion of fibers particles (reinforcements). Their water absorption rate varies between 128.00% and 602.60%, and the absorption rate of the various foams decreases with increasing density, indicating a high affinity for water. The Young's modulus of the various foams varies between 0.21 and 1.14 MPa. It can be seen that their strength increases with the level of reinforcement. Higher-density foams normally resist compression more than lower-density foams. These results enabled us to classify this foam as a rigid foam and to note that the fiber content influences the characteristics of the foam.

**Keywords:** Rigid foam; tannin; sugar cane bagasse; raffia bamboo cork; chemical characteristics; thermal characteristics.

Date of Submission: 13-12-2024

Date of acceptance: 28-12-2024

### 1. INTRODUCTION

Since ancient times, people have sought to improve their living conditions. Since the end of the 20th century, this quest for better living conditions has taken off. During this period, increasingly high-performance materials, including foams, were developed.

With oil prices on the rise and the scarcity of oil predicted for the coming years, various research teams are working on the use of natural resources to replace petrochemical-based products. As a result, natural raw materials such as tannins have been incorporated into a

wide range of applications. These tannins are obtained from wood and/or bark [1], [2].

Foams are generally produced by releasing a gas into a high-viscosity liquid medium that hardens as the gas escapes [3]. Examples can be found in everyday life, such as bread or most cakes. But solid foams can also be produced by hardening a polymer. Latex mattresses, polyurethane foam sofas, and polyurethane foams for the soles of sports shoes are all examples of how foam technology is adapted to human life.

Rigid tannin foams are obtained by polycondensation of polyflavonoid tannins with furfuryl alcohol. These foams can have a wide range of

characteristics, depending on their density and the type of additives used.

As part of this drive to use more and more natural products, researchers are now looking into the possibility of incorporating tannins into the resin used to manufacture natural fiber-reinforced materials, in order to increase the percentage of natural and renewable products. [4].

Wedaina et al. (2020) showed that Monopetalantus tannin is a condensed tannin with good properties for producing bio-composites.

However, a thorough laboratory analysis is necessary to ascertain the thermomechanical properties of a composite material before it can be used in various industrial sectors, including construction, automotive, and aerospace. Because they don't distort, rigid foams are typically utilized in buildings for acoustic and thermal insulation. Because of their lightweight nature and capacity to absorb mechanical energy and stress, rigid foams are occasionally used as shock absorbers in automobiles.

Working on the assumption that the combined materials should give rise to a composite with properties better than those of each material, with the aim of better appreciating the characteristics of the composite, this work will be based on the following hypotheses: sugarcane bagasse fibers and raffia cork fibers could be used in the manufacture of tannin-based foams, the foam obtained could have various applications, the variation in the fiber content would influence the thermomechanical characteristics of the rigid tannin-based foam. The main objective of this study will therefore be to investigate the effect of adding different proportions of fiber particles to a tannin-based foam on its thermomechanical properties.

The development protocol adopted is that of Tondi and Pizzi (2009) [5]. However, it should be noted that formaldehyde is a product that is harmful to health and the environment, so we chose to reduce the quantity of this product by adding *Vachellia nilotica*, a natural hardener, to overcome this problem [6].

## 2. MATERIALS AND METHODS

### 2.1. Acquisition and processing of Ekop-mayo (*Monopetalantus*) bark

Ekop-mayo were collected from several timber harvesting companies located in Yassa in the city of Douala in the Littoral Region of Cameroon (Latitude: 4°02'53" North, Longitude: 9°42'15" East). As the bark was not very dry when it was collected, we dried it in the sun for a month, after which it was ground into a fine powder to make it easier to use.

### 2.2. Tannin extraction

2865 g of fine Ekop-mayo bark powder, 57,3 g of bisulfite, 14.35 g of bicarbonate, and 17910 g of water were used to extract the tannins. A mass M1 of crushed wood bark powder is poured into a pot containing a volume V2 of water 2% sodium

meta-bisulphite and 0.5% sodium bicarbonate. The volume of water used is equal to 6 times the mass of wood bark calculated on the dry mass, and the masses of meta-bisulphite and sodium bicarbonate are calculated in relation to the mass of wood bark (powder) used and weighed using a digital balance. The mixture was then placed in a pickling bath heated to 60°C with stirring for 4 hours. Then the whole is filtered to obtain a reddish-black liquid filtra. The liquid fraction recovered is then concentrated using a rotary evaporator at a temperature of 60 °C. This yields tannin in viscous form, which is oven-dried at 50 °C for 48 hours [7].

### 2.3. Cane bagasse extraction

The sugar cane bagasse was collected from markets in Douala, dried in the sun for a fortnight and then ground into very short fibers.

### 2.4. Extraction of cork fibers from raffia bamboos

The raffia bamboo was collected from a raffia field in the West Cameroon region (latitude 5°32'09.60" North and longitude 10°34'22.80" East) and then dried for 14 days. The outer part of the bamboo was cut with a knife. The bamboo obtained was cut into small pieces using a machete and then, using a mechanical grinder, the bamboo fibers were obtained. After grinding, the resulting product was sieved using 1.00 mm mesh sieves. Figure 4 shows the process for obtaining raffia bamboo fibers.

### 2.5. Extraction of bio-hardener

A knife was used to scratch the bark of a *Vachellia nilotica* tree in several places. The scratches were between 0.5 and 1 centimeter deep. After 30 minutes, the exiting sap was collected and then dried at room temperature (37°C) for 21 days. The dried exudates consisted specially of 2-hydroxy-5-hydroxymethyl furan and especially 2,5-dihydroxymethyl furan [6], were ground to obtain a whitish soluble powder.

### 2.6. Protocol for producing tannin-based rigid foam

A mass M1 of tannin powder is mixed with X ml of furfuryl alcohol and a mass M2 of fibers of (cane bagasse or bamboo) in aqueous solution (water) in a mould under strong mechanical agitation using a manual glass stirrer. The 37% formaldehyde is then added with the *Vachellia nilotica* exudate. After 20 seconds of stirring, the mixture of diethyl ether + 65% para-toluene sulphonic acid in distilled water was added. The resulting solution is placed in an oven at 40°C for 24 hours to allow the foam to form and mature. This foam is left to rest for 5 days before their characterization. The quantities of reagents used were measured using a 1/1000° digital balance.

The quantities of reagents used to produce tannin foam are given in Tables 1, 2 and 3.

**Table 1:** Coding used to produce foam

<b>Foams</b>	<b>Meaning</b>
<b>M0</b>	Tannin foam without reinforcement, containing 50% formaldehyde and 50% bio-hardener.
<b>MBC0</b>	Tannin foam reinforced with sugar cane bagasse fiber (0.2 g; i.e. 1.66% of the tannin mass) and also containing 50% formaldehyde and 50% bio-hardener.
<b>MBC1</b>	Tannin foam reinforced with sugar cane bagasse fiber (0.3 g, i.e. 2% of the tannin mass) and also containing 50% formaldehyde and 50% bio-hardener.
<b>MBC2</b>	Tannin foam reinforced with sugar cane bagasse fiber (0.6 g; i.e. 4% of the tannin mass) and also containing 50% formaldehyde and 50% bio-hardener.
<b>MLR0</b>	Tannin foam reinforced with raffia cork fibers (0.2 g; i.e. 1.66% of the tannin mass) and containing 50% formaldehyde and 50% bio-hardener.
<b>MLR1</b>	Tannin foam reinforced with raffia cork fibers (0.3 g, i.e. 2% of the tannin mass) and containing 50% formaldehyde and 50% bio-hardener.
<b>MLR2</b>	Tannin foam reinforced with raffia cork fibers (0.6 g; i.e. 4% of the tannin mass) and containing 50% formaldehyde and 50% bio-hardener.

The following proportions were used to produce the foam.

**Table 2:** *Raffia cork foam*

<b>Elements/foams</b>	<b>M0</b>	<b>MLR1</b>	<b>MLR2</b>	<b>MLR3</b>
<b>Tannin (g)</b>	15	15	15	15
<b>Fiber (g)</b>	-	<b>0.2</b>	<b>0.3</b>	<b>0.6</b>
<b>AF (g)</b>	5.2	5.2	5.2	5.2
<b>Distilled water (g)</b>	3	3	3	3
<b>Formaldehyde</b>	1.85	1.85	1.85	1.85
<b>Natural hardener</b>	1.85	1.85	1.85	1.85
<b>PTSA 65% (g)</b>	6	6	6	6
<b>DE (g)</b>	2	2	2	2

**Table 3: Sugar cane bagasse foam**

Elements/foams	M0	MBC1	MBC2	MBC3
Tannin (g)	15	15	15	15
Fiber (g)	-	0.2	0.3	0.6
AF (g)	5.2	5.2	5.2	5.2
Distilled water (g)	3	3	3	3
Formaldehyde	1.85	1.85	1.85	1.85
Natural hardener	1.85	1.85	1.85	1.85
PTSA 65% (g)	6	6	6	6
DE (g)	2	2	2	2

## 2.7. ATR-FTIR analysis of tannin and fibers from bamboo and sugarcane bagasse

A Fourier Transform Infrared Spectroscopy, Nicolet Nexus 870 was used to analyze the chemical structure of raffia bamboo fibers, sugarcane bagasse and *Monopetalantus* tannin powder. Experimental spectra ranged from 4000 to 400  $\text{cm}^{-1}$  with a resolution of 2  $\text{cm}^{-1}$  using KBr pellets, equipped with an attenuated total reflection (ATR) accessory (Thermo Fisher Scientific Inc., Waltham, MA). Duplicate spectra were recorded for each sample. The ATR crystal was made of diamond and had an angle of incidence of 45°. For ATR-FTIR analysis, approximately 1mg of *Monopetalantus* tannin powder followed by 1mg bamboo raffia fibers and 1mg sugarcane bagasse were successively placed on the ATR crystal to cover the diamond surface and the press was lowered to apply pressure to the sample to form a close interaction surface between the sample and the diamond surface.

## 2.8. Characterization of tannin foams

### 2.8.1. TGA-DSC analysis

Thermal analysis was carried out on a Linseis STAPT- 1000 asynchronous thermogravimetric analyzer with a resolution of 0.5  $\mu\text{g}$  connected to a computer and controlled by platinum Evaluation V.1.0 software. 182 capable of combining thermogravimetry (TG) and differential scanning calorimetry (DSC) information on the same samples. Approximately 3 to 5mg of fiber powder were placed in a platinum crucible and then heated in the furnace at a constant heating rate of 10°C/min over a temperature range of 25°C to 700°C under a flow of nitrogen at a rate of 50ml/min.

### 2.8.2. Apparent density

The apparent density ( $\rho_{ap}$ ) of rigid foam was determined using a calliper to obtain the dimensions of the parallelepiped test specimens and a balance to weigh the specimens. The apparent density is obtained using the following formula Eq. (1):

$$\rho_{ap} = \frac{m_{ap}}{U_{ap}} \quad (1)$$

With:

$\rho_{ap}$  is bulk density

$m_{ap}$  is apparent mass

$U_{ap}$  is apparent volume

### 2.8.3. Water absorption rate

The absorption rate ( $T_A$ ) was determined in accordance with standard NFG08-012. After weighing the test tubes using a 1/1000 digital balance, the samples were placed in a jar filled with distilled water and left submerged for 24 hours. The samples were then removed from the water and dried with a cloth before being weighed again, or simply drained for a few minutes and the masses recorded. The water absorption of the samples was determined using the formula Eq. (2):

$$T_A = \frac{m_a - m_i}{m_i} \times 100 \quad (2)$$

With:

$T_A$ : The absorption rate

$m_i$ : initial masse of the dry sample

$m_a$ : masse of sample after submerged in water for 24h

#### 2.8.4. Compression test

Compressive strength tests were carried out on a 3R BED -100 universal testing machine (Figure 1) at the Upper Room Institute located at AKWA in the city of Douala.) This machine is controlled by a computer. Its maximum force cell is 1000 N and the maximum crosshead speed is 6.0mm/min.

The specimen, measuring 30×30×15 (in mm), was placed between two circular compression plates. The specimen was compressed until it was flattened using the upper plate at a constant speed of 0.1mm/s. During the experiments, the force and displacement of the crosshead were recorded in an Excel table.

### 3. RESULTS AND DISCUSSION

#### 3.1. Tannin extraction yield

After extraction, the mass of tannin obtained was weighed. This mass gave a value of 257.63g. This gives a yield of 8.99%. For a mass of 2865 g of ekop-mayo bark, 257.63 g of tannin was obtained. This is certainly due to the fact that all impurities were removed during the filtering process.

#### 3.2. ATR-FTIR analysis of tannins, bamboo raffia fibers and sugar cane bagasse fibers

- Analysis of the ATR-FT IR spectrum of *Ekop mayo (Monopetalantus)* tannin

Figure 5 shows the ATR-FT MIR spectrum of Ekop mayo (*monopetalantus*) tannin extract studied in the fingerprint (4000 - 400  $\text{cm}^{-1}$ ).

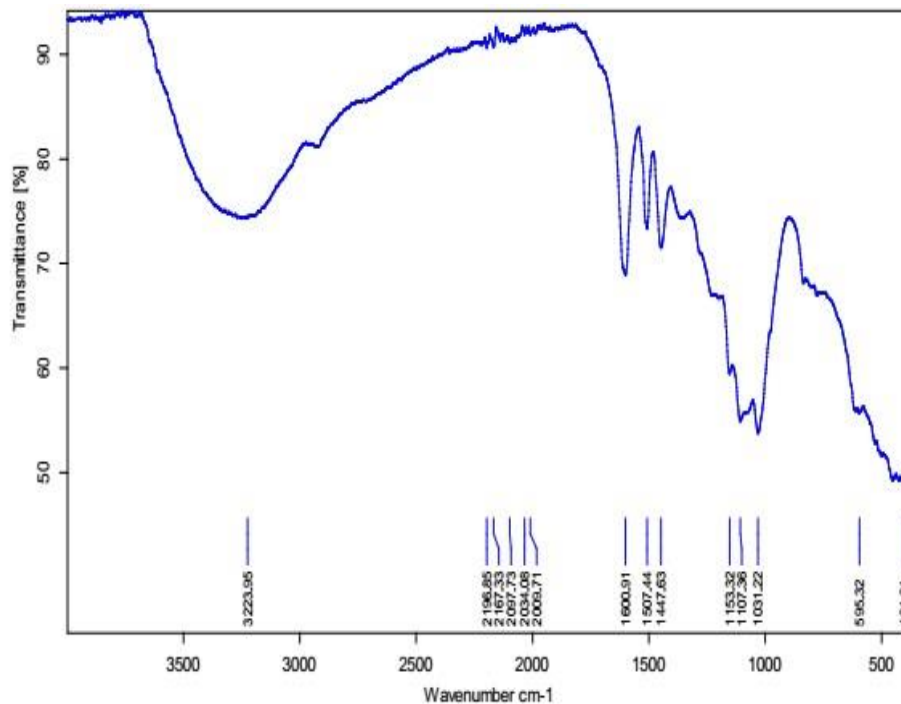


Figure 2: ATR-FT spectrum of Ekop mayo tannin extract (*Monopetalantus*)



Figure 1: compression test set-up

Analysis of the ATR-FT spectrum of Monopetalantus tannin extract (figure 2) in the range  $4000 - 400 \text{ cm}^{-1}$  reveals the existence of several functional groups specific to condensed and hydrolysable tannins: before distinguishing between the existence of these two families of tannins, it is interesting to note that bands specific to both families of tannins attributed to benzene hydroxyl groups are identified in this extract. Peaks  $1447$  and  $1031 \text{ cm}^{-1}$  are considered the most significant and sufficient to describe the presence of the benzene nucleus. The  $1447 \text{ cm}^{-1}$  peak is attributed to the bending of aromatic compounds in general and the  $1031 \text{ cm}^{-1}$  peak results from the combination of C-H bond bending, C-O stretching and C-OH bond deformations of the aromatic components [8]. The shoulder located around  $1153 \text{ cm}^{-1}$  is associated with in-plane bending of the C-H bonds of the aromatic compounds [3].

It is possible to distinguish the existence of two families of tannin in this extract: the presence of condensed tannin is justified not only by the presence of the  $1600 \text{ cm}^{-1}$  peak, a peak specific to proanthocyanidins [9] which is generally occupied by the vibrations of the C=C bonds of the aromatic ring, but also by the stretching of the C-O bonds present at peaks  $1153$  and  $1031 \text{ cm}^{-1}$ . These last two peaks represent the stretching of the C-O-C bonds of the C core of flavonoids [10]. The peak located at  $595 \text{ cm}^{-1}$  is attributed either to torsion of the A ring of flavonoids, or to flavan, flavanol, pyrocatechol, resorcinol, epicatechin, or to the hydroxyl group of aromatic compounds or in-plane bending of the CH bonds of aromatic compounds or to esters. These esters can be attributed to the gallic acid generally associated with catechin/epicatechin or epicatechin gallate present in procyanidins or to the deformation of the  $\text{CH}_2 - \text{OH}$  groups of carbohydrate residues.

#### - Analysis of the ATR-FT IR spectrum of sugarcane bagasse and bamboo fibers

The infrared absorption spectrum of sugarcane bagasse can be seen in Figure 3.

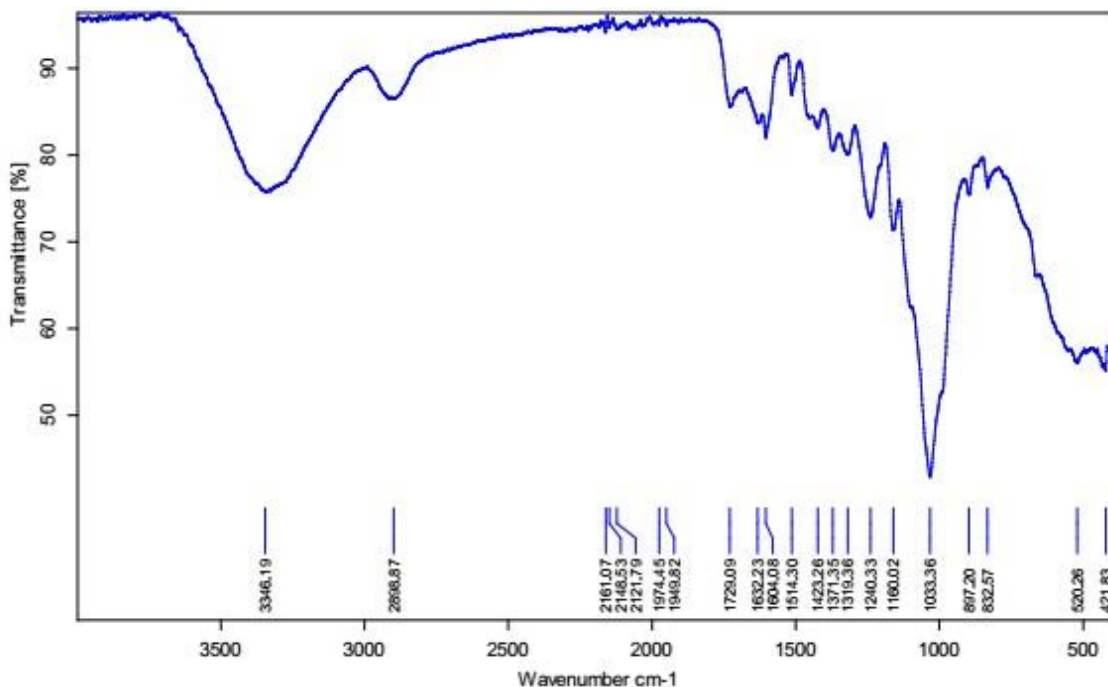


Figure 3: Sugar cane bagasse

The main characteristics are attributed to the presence of lignin, hemicellulose and cellulose, which are characteristic of natural fibers. In general,

infrared spectra for native fibers are representative in the spectral range  $3200-3600 \text{ cm}^{-1}$ . At  $2.898 \text{ cm}^{-1}$ ,

the absorption band observed is linked to axial deformation of the C-H group. The peak at 1729  $\text{cm}^{-1}$  is linked to the axial deformation of the C-H group, characteristic of the carbonyl (C=O) band of the hemicellulose in sugarcane bagasse. The band at 1423  $\text{cm}^{-1}$  is representative of the

symmetrical deformation of the  $\text{CH}_2$  group in cellulose, while the band at 1243  $\text{cm}^{-1}$  refers to the C-O-C group in the cellulose chain. The band at 1151  $\text{cm}^{-1}$  is related to the asymmetric deformation of the  $\text{CH}_2$  group in cellulose linked to the asymmetric deformation of the C-O-C group in cellulose and hemicellulose.

The absorption spectrum for bamboo fibers shows certain similarities with that for sugar cane bagasse (Figure 4).

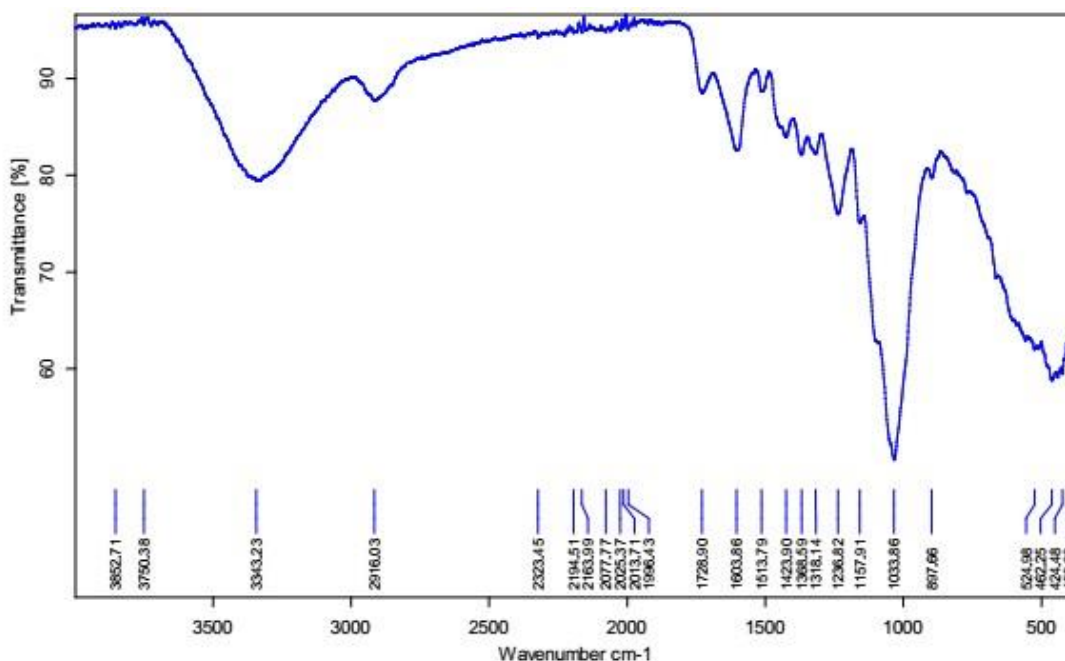


Figure 4: Bamboo raffia

At 2916  $\text{cm}^{-1}$  the band is linked to axial deformation of the C-H group, while the band at 2163  $\text{cm}^{-1}$  is linked to C=C stretching vibrations. The carbonyl group of hemicelluloses gives a signal at 1603  $\text{cm}^{-1}$ , while the band at 1236  $\text{cm}^{-1}$  is associated with the presence of C-O-C in the cellulose chain. The strong absorption band at 1038  $\text{cm}^{-1}$  is linked to the C-OH stretching vibration.

### 3.3. Characteristics of tannin foams

#### 3.3.1. TGA-DSC analysis

The thermal properties were measured by TGA, where it was observed that the M0 foam (Figure 5) degraded completely at around 480°C. However, for the MBC1 foam (Figure 6), and the MLR1 foam (Figure 7), it appears respectively that

around 2.81% and 6.99% of the sample degraded at around 500°C, which is probably the foam part; from 11.45% the water starts to disappear and from 200°C, the material starts to lose its mouldings. Consequently, it seems that resistance to thermal degradation is provided by the reinforcement of the fibres and the presence of the bio-hardener. It was assumed that the bio-hardener would protect against thermal degradation because it consists of furan [11] which would provide fire retardancy to the rigid foam by carbonising instead of burning. However, since tannin foam is already known to have a high degree of fire retardancy, the added formaldehyde and bio-hardener did not cause any difference in thermal stability [12].

After analysing the DSC spectra, it was observed that at the first heat (Figure 5), the tannin extract and the foam showed similar thermal transitions

at 300°C, which shows that the thermal transition in the foam is probably due to the tannin extract and, in turn, to the condensation and rearrangement reactions of the tannin extract. In the second heat, the MO foam showed a thermal transition at 438°C (Figure 5) while the MLR1 foam showed two

exothermic peaks at 386°C and 426°C (Figure 6), and the MBC1 foam showed an exothermic peak at 411°C (Figure 6), indicating a condensation reaction, prior to 400°C. This illustrates that the foams have a condensation reaction. This illustrates that the foams have no detectable residual monomer in the polymer structure.

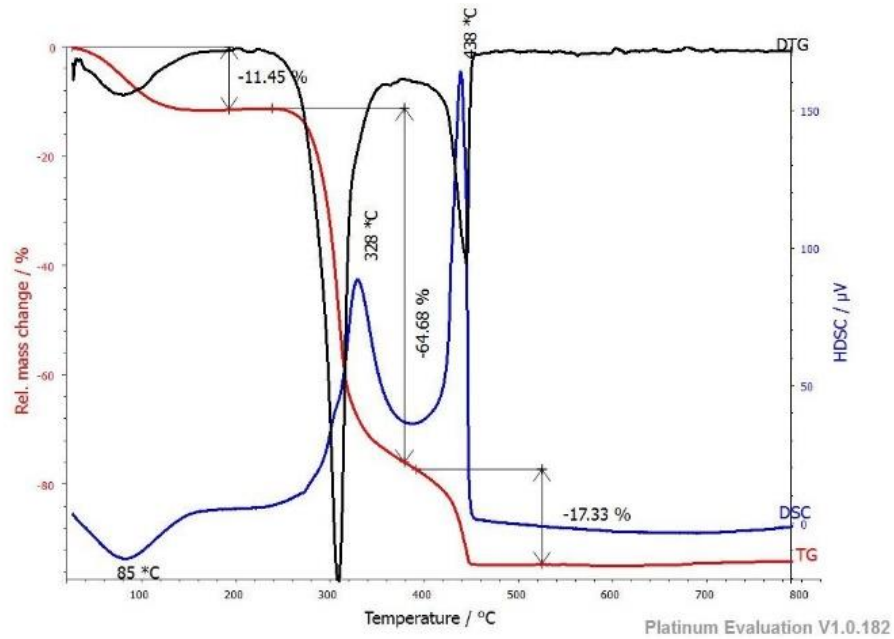


Figure 5: Tannin foam (M0)

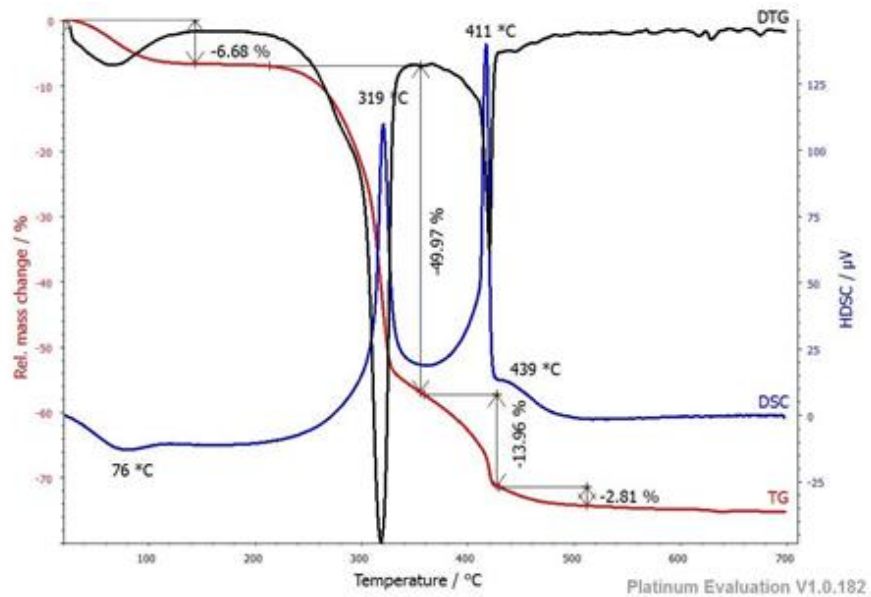


Figure 6: Sugar cane bagasse foam (MBC1)



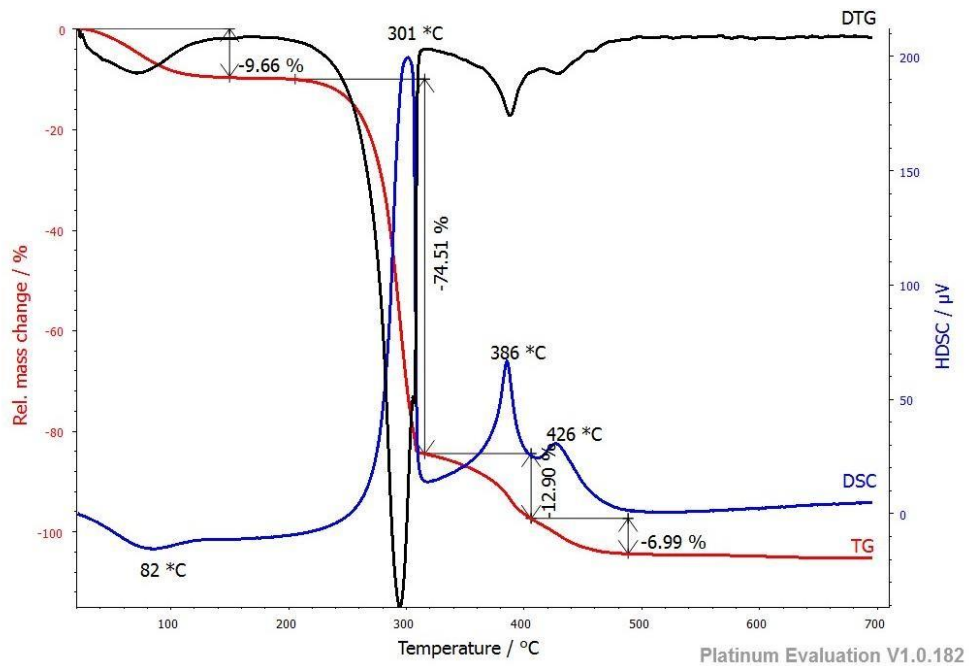


Figure 7: Bamboo raffia cork foam

### 3.3.2. Apparent density

Table 4 shows the data used to obtain the bulk density.

Table 4: Data for calculating bulk density

	M0	MBC0		MBC1		MLR0		MLR1	
	M0	MBC0	MBC0	MBC1	MBC1	MLR0	MLR0	MLR1	MLR1
Mass (g)	1.17	1.86	1.88	20.51	3.66	5.01	4.63	5.35	5.05
Volume (cm <sup>3</sup> )	13.5	11.7	11.7	101.81	9	10.8	9.9	9.126	9.72
Density (g/cm <sup>3</sup> )	0.086	0.158	0.160	0.201	0.406	0.463	0.467	0.586	0.519
Average (g/cm <sup>3</sup> )	0.086	0.159		0.304		0.465		0.552	

Analysis of the results in Table 4 shows that the density of M0 foam is 0.08 g/cm<sup>3</sup>; that of MBC foams varies between 0.15 and 0.3 g/cm<sup>3</sup>; and that of MLR foams varies between 0.46 and 0.47 g/cm<sup>3</sup>. The highest values were recorded for MBC1 and MLR1 foams. This behaviour may be due to the fact that the density of bamboo and sugarcane bagasse predominates over that of the base resin respectively.

It was found that the apparent density of M0 foam is 0.08 g/cm<sup>3</sup> which is the same density as Tondi et al. (2009). Furthermore, the density increases with the proportion of fiber particles (reinforcements).

### 3.3.3. Water absorption rate

Table 5 shows the various data used to obtain water absorption.

**Table 5:** Data table for obtaining water absorption

	M0		MLR0		MLR1		MBC0		MBC1	
Samples	M01	M02	MLR01	MLR02	MLR11	MLR12	MBC01	MBC02	MBC11	MBC12
<b>Initial mass (g)</b>	1.2	1.17	5.01	4.24	4.27	4.86	2.23	1.86	3.66	3.69
<b>final mass (g)</b>	8.76	7.9	11.1	10.87	9.86	10.94	11.11	10.55	10.98	12.82
<b>AR (%)</b>	630	575.2	121.56	156.37	131	125.1	398.21	467.2	200	247.43
<b>Average AR</b>	<b>602.60 ± 27</b>		<b>138.96 ± 17</b>		<b>128 ± 2</b>		<b>432.70 ± 34</b>		<b>223.71 ± 23</b>	

An analysis of the results in Table 5 shows that the absorption rate for M0 foams is 602.61%; that for MBC foams varies between 138.96 and 128.00%; and that for MLR foams varies between 432.7 and 223.71%. The highest values were recorded for M0 foams. This behaviour can be explained by the fact that bamboo fibers and sugarcane bagasse fibers do not absorb enough water.

This result shows that foam without reinforcement has a higher absorption rate than other foams (with reinforcement). Also, the higher the level of reinforcement, the lower the absorption rate of the foam.

### 3.3.3.1. Influence of density on absorption rate

Analysis of the data in Figure 11 shows that the absorption rate decreases with increasing density. The greater the density of the foam, the less water it absorbs. The more the foam is reinforced, the greater its density, resulting in fewer pores. This would explain the reduced water absorption of these foams.

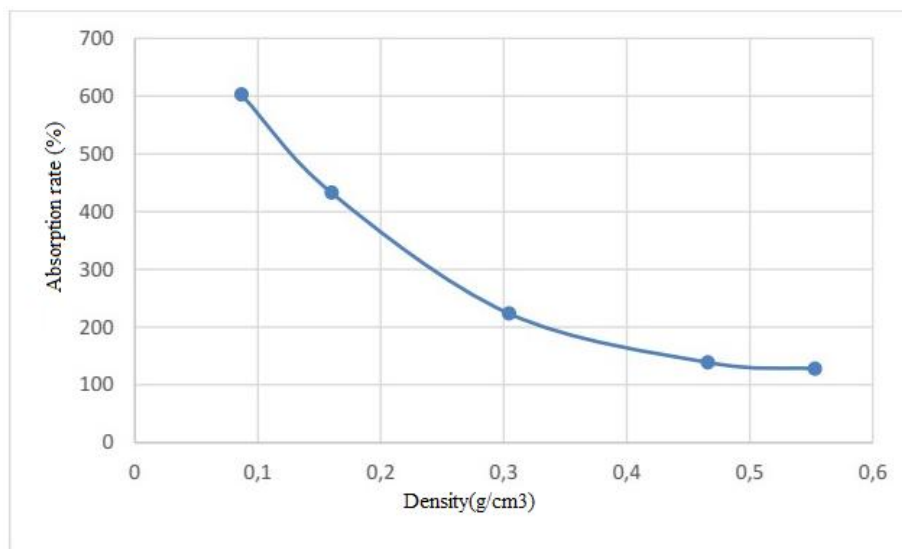


**Figure 8:** Changes in density as a function of absorption rate

### 3.4. Compression characteristics of foams

After subjecting the M0, MBC0, MBC1, MLR0 and MLR1 foams to the

compression test, stress versus strain curves were obtained (Figure 9).

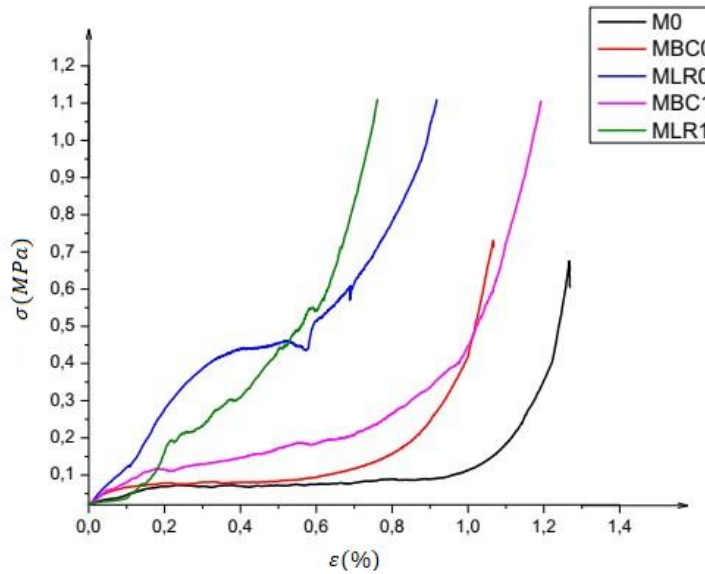


Figure 9: Curves for compression testing of tannin foams

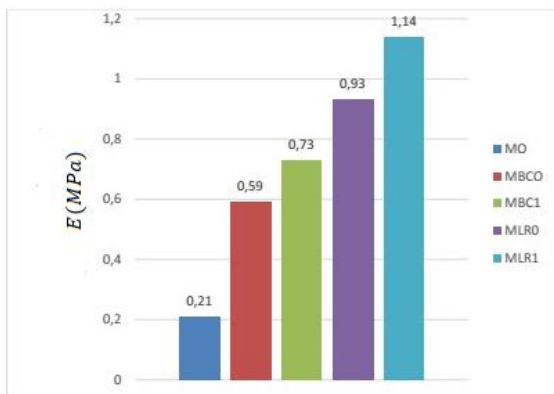


Figure 10: a) Young's modulus distribution

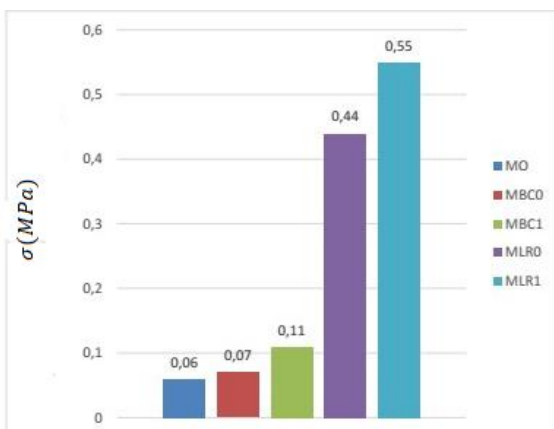


Figure 10: b) Compressive strength distribution

Analysis of the data in Table 9 and Figure 10 (a and b) shows that the compressive strength of M0 foams is 0.06 MPa; that of MBC foams varies between 0.07 and 0.11 MPa; and that of MLR foams varies between 0.44 and 0.55 MPa. The Young's modulus of M0 foams is 0.21MPa; that of MBC foams varies between 0.59 and 0.73 MPa; that of MLR foams varies between 0.93 and 1.14 MPa.

The highest values were recorded for MBC1 and MLR1 foams. This behaviour can be explained by the fact that bamboo fibers and cane bagasse fibers resist compression, which would explain these results.

This shows that strength and Young's modulus increase with the level of reinforcement. Higher-density foams normally resist compression more than lower-density foams.

### 4. CONCLUSION

In conclusion, this study aimed to evaluate the influence of fiber particle content on a rigid foam based on Monopetalantus tannin. To achieve this, the extraction and chemical characterization of the tannin, sugarcane bagasse fibers, bamboo cork fibers, and the bio-hardener Vachellia nicoleta were first carried out. Then, foam samples were prepared by varying the particle content, and they were physically and mechanically characterized. This study highlighted the different properties of the foams produced.

It was found that higher density foams resist compression better than lower density ones, and that the Young's modulus of the foams increases with the reinforcement content.

## REFERENCES

- [1]. Ndiwe, B., Tibi, B., Danwe, R., Konai, N., Pizzi, A., Amirou, S., 2020. Reactivity, characterization and mechanical performance of particleboards bonded with tannin resins and bio hardeners from African trees. *International Wood Products Journal* 11, 80-93.
- [2]. Wedaïna, A.G., Pizzi, A., Nzie, W., Danwe, R., Konai, N., Amirou, S., Segovia, C., Kueny, R., 2021. Performance of unidirectional biocomposite developed with Piptadeniastrum Africanum tannin resin and Urena Lobata fibers as reinforcement. *Journal of Renewable Materials* 9, 477-493.
- [3]. Athomo, A.B.B., Anris, S., Tchiana, R.S., Eyma, F., de Hoyos-Martinez, P., Charrier, B., 2020. Biobased adhesives from African mahogany tannins : Characterization by 1H and 13C NMR and physicochemical properties. *Global Journal of Botanical Science* 8, 11-20.
- [4]. Hussin, M.H., Abd Latif, N.H., Hamidon, T.S., Idris, N.N., Hashim, R., Appaturi, J.N., Brosse, N., Ziegler-Devin, I., Chrusiel, L., Fatriasari, W., others, 2022. Latest advancements in high- performance bio-based wood adhesives: A critical review. *Journal of Materials Research and Technology* 21, 3909-3946.
- [5]. Tondi, G., Pizzi, A., 2009. Tannin-based rigid foams: Characterization and modification. *Industrial crops and Products* 29, 356-363.
- [6]. Ndiwe, B., Pizzi, A., Tibi, B., Danwe, R., Konai, N., Amirou, S., 2019. African tree bark exudate extracts as biohardeners of fully biosourced thermoset tannin adhesives for wood panels. *Industrial Crops and Products* 132, 253-268. <https://doi.org/10.1016/j.indcrop.2019.02.023>
- [7]. Nga, L., Ndiwe, B., Biwolé, A.B., Pizzi, A., Biwole, J.J.E., Mfomo, J.Z., 2024. Matrix Assisted Laser Desorption Ionization Time of Flight (MALDI-TOF)-Mass Spectrometry and <sup>13</sup>C-NMR-Identified New Compounds in Paraberlinia bifoliolata (Ekop-Beli) Bark Tannins. *JRM* 12, 553-568. <https://doi.org/10.32604/jrm.2023.046568>
- [8]. Basso, M.C., Pizzi, A., Maris, J.P., Delmotte, L., Colin, B., Rogaume, Y., 2017. MALDI- TOF, 13C NMR and FTIR analysis of the cross-linking reaction of condensed tannins by triethyl phosphate. *Industrial crops and products* 95, 621-631.
- [9]. Chupin, L., Motillon, C., Charrier-El Bouhtoury, F., Pizzi, A., Charrier, B., 2013. Characterisation of maritime pine (Pinus pinaster) bark tannins extracted under different conditions by spectroscopic methods, FTIR and HPLC. *Industrial Crops and Products* 49, 897-903.
- [10]. Nardeli, J.V., Fugivara, C.S., Taryba, M., Montemor, M., Ribeiro, S.J., Benedetti, A.V., 2020. Novel healing coatings based on natural-derived polyurethane modified with tannins for corrosion protection of AA2024- T3. *Corrosion Science* 162, 108213.
- [11]. Ndiwe, B., Pizzi, A., Chapuis, H., Konai, N., Karga, L., Girods, P., Danwe, R., 2022. Desorption Behavior and Thermogravimetric Analysis of Bio-Hardeners. *Journal of Renewable Materials* 10, 2015-2027. <https://doi.org/10.32604/jrm.2022.019891>
- [12]. Kumar, C., Leggate, W., 2022. An overview of bio-adhesives for engineered wood products. *International Journal of Adhesion and Adhesives* 118, 103187.